

# Metamaterial based telemetric strain sensing in different materials

Rohat Melik<sup>1\*</sup>, Emre Unal<sup>1</sup>, Nihan Kosku Perkgoz<sup>1</sup>, Christian Puttlitz<sup>2</sup>, and Hilmi Volkan Demir<sup>1</sup>

<sup>1</sup> Departments of Electrical Engineering and Physics, Nanotechnology Research Center, and Institute of Materials Science and Nanotechnology, Bilkent University, Ankara, 06800, Turkey;

<sup>2</sup> Department of Mechanical Engineering and School of Biomedical Engineering, Orthopaedic Bioengineering Research Laboratory, Colorado State University, Fort Collins, CO 80523, USA

\*rohat@ee.bilkent.edu.tr

**Abstract:** We present telemetric sensing of surface strains on different industrial materials using split-ring-resonator based metamaterials. For wireless strain sensing, we utilize metamaterial array architectures for high sensitivity and low nonlinearity-errors in strain sensing. In this work, telemetric strain measurements in three test materials of cast polyamide, derlin and polyamide are performed by observing operating frequency shift under mechanical deformation and these data are compared with commercially-available wired strain gauges. We demonstrate that hard material (cast polyamide) showed low slope in frequency shift vs. applied load (corresponding to high Young's modulus), while soft material (polyamide) exhibited high slope (low Young's modulus).

©2010 Optical Society of America

**OCIS codes:** (160.3918) Metamaterials; (280.0280) Remote sensing and sensors.

---

## References and links

1. A. Ghali, and R. Favre, Concrete Structures: Stresses and Deformations (E & FN Spon, London, 1994).
2. R. Melik, N. K. Perkgoz, E. Unal, C. Puttlitz, and H. V. Demir, "Bioimplantable passive on-chip RF-MEMS strain sensing resonators for orthopaedic applications," *J. Micromech. Microeng.* **18**(11), 115017 (2008).
3. R. Melik, E. Unal, C. Puttlitz, and H. V. Demir, "Metamaterial-based wireless strain sensors," *Appl. Phys. Lett.* **95**(1), 011106 (2009).
4. H. Chen, B.-I. Wu, B. Zhang, and J. A. Kong, "Electromagnetic wave interactions with a metamaterial cloak," *Phys. Rev. Lett.* **99**(6), 063903 (2007).
5. R. A. Shelby, D. R. Smith, and S. Schultz, "Experimental verification of a negative index of refraction," *Science* **292**(5514), 77–79 (2001).
6. S. Zhang, W. Fan, B. K. Minhas, A. Frauenglass, K. J. Malloy, and S. R. J. Brueck, "Midinfrared resonant magnetic nanostructures exhibiting a negative permeability," *Phys. Rev. Lett.* **94**(3), 037402 (2005).
7. V. M. Shalaev, "Optical negative-index metamaterials," *Nat. Photonics* **1**(1), 41–48 (2007).
8. C. G. Parazzoli, R. B. Greigor, K. Li, B. E. C. Koltenbah, and M. Tanielian, "Experimental verification and simulation of negative index of refraction using Snell's law," *Phys. Rev. Lett.* **90**(10), 107401 (2003).
9. J. D. Wilson, and Z. D. Schwartz, "Multifocal flat lens with left-handed metamaterial," *Appl. Phys. Lett.* **86**(2), 021113 (2005).
10. A. Salandrino, and N. Engheta, "Far-field subdiffraction optical microscopy using metamaterial crystals: Theory and simulations," *Phys. Rev. B* **74**(7), 075103 (2006).
11. M. S. Rill, C. Plet, M. Thiel, I. Staude, G. von Freymann, S. Linden, and M. Wegener, "Photonic metamaterials by direct laser writing and silver chemical vapour deposition," *Nat. Mater.* **7**(7), 543–546 (2008).
12. G. Dolling, C. Enkrich, M. Wegener, C. M. Soukoulis, and S. Linden, "Simultaneous negative phase and group velocity of light in a metamaterial," *Science* **312**(5775), 892–894 (2006).
13. <http://www.mathweb.com>

---

## 1. Introduction

Measuring strain telemetrically presents a large industrial challenge [1,2]. To address this problem, we developed a metamaterial based wireless strain sensing method that monitors strain in real time by observing the operating frequency ( $f_0$ ) shift under varying levels of strain [3]. The current work extends these preliminary findings to different industrial materials to demonstrate the applicability of incorporating metamaterials for widespread applications.

The operating principle of our sensing approach is that when a force is applied to the sensor, the operating frequency of the metamaterial sensor is shifted, and, by observing this frequency change ( $\Delta f_0$ ), we can monitor the strain in real time. In order to have an efficient wireless strain sensor working with this guiding principle, one must have the ability to easily measure the operating frequency. Thus, the sensor must provide a relatively high local minimum and sufficient sharpness at the minimum. Other desirable properties are high sensitivity and low nonlinearity-error with loading. If the sensitivity is too low, then the shift of operating frequency will be insufficient and the strain will not be detectable. If there is too much nonlinearity-error, then accurately relating the operating frequency to strain involves a more complicated readout process. The employment of metamaterials for use in the manufacture of wireless strain sensors is advantageous because of their unique structural properties. Metamaterials have gaps (splits) that have higher electric field intensity localization compared to conventional radio frequency (RF) – micro-electro-mechanical systems (MEMS) sensing structures. Hence, they yield higher signal-to-noise ratios, which results in better linearity. These additional gaps also yield greater relative deformation, which leads to better sensitivity. Since metamaterials demonstrate higher sensitivity and lower nonlinearity-errors as compared to other conventional RF-MEMS sensing structures, we propose that metamaterials can be used for widespread wireless strain sensing applications in industry.

There are many proposed applications areas for metamaterials. Some of these applications include cloaking [4], negative refractive index [5–8], focusing light [9], subwavelength resolution [10] and laser manufacture [11,12]. We have previously reported using metamaterials in the manufacture of telemetric sensors [3] for detecting mechanical strain telemetrically in real time. In this paper, using test materials of cast polyamide, derlin and polyamide, we apply compressive loads to our sensors and observe significant operating frequency shifts with the deformation of these test materials. These data are compared to strain measurements using traditional, commercial wired strain gauges on the same test materials. In this paper, different from our previously published paper [3], we study wireless sensors for different Young's modulus of materials telemetrically and show that they exhibit different slopes in the behavior of their frequency shift *vs.* the applied load (corresponding to different levels of Young's modulus). In addition to showing proof-of-concept demonstrations of using metamaterials in widespread areas of industry where wireless strain sensing is required, we also present a different method for monitoring Young's modulus remotely by observing different slopes in *f vs. load* characterization (e.g., for the purpose of monitoring and assessment of fracture healing). Monitoring such an evolution of this slope in *f vs. load* for an implantable plate at different times potentially offers surgeons the ability to follow different phases of healing process remotely.

## 2. Fabrication and experimental characterization

The metamaterial sensor fabrication starts with depositing  $0.1\ \mu\text{m}$   $\text{Si}_3\text{N}_4$  onto our silicon substrate via plasma enhanced chemical vapor deposition (PECVD) and is followed by lithography of our metamaterial pattern of split ring resonator array. Subsequent metallization using a box-coater allows for deposition of  $0.1\ \mu\text{m}$  Au to obtain the final structure. Figure 1 shows the sensors adhered to the test materials of cast polyamide (in Fig. 1(a)), derlin (in Fig. 1(b)), and polyamide (in Fig. 1(c)). Each sensor chip has  $5 \times 5$  repeating unit cells, yielding a  $1.5\ \text{cm} \times 1.5\ \text{cm}$  total chip size. Each sensing unit has a  $2220\ \mu\text{m}$  outer length denoted as  $L_{\text{out}}$  and a  $1380\ \mu\text{m}$  inner length denoted as  $L_{\text{in}}$ , with  $140\ \mu\text{m}$  inner ( $w_{\text{in}}$ ) and outer ( $w_{\text{out}}$ ) widths, and  $280\ \mu\text{m}$  inner ( $s_{\text{in}}$ ) and outer ( $s_{\text{out}}$ ) spacings. The repeating length of this unit cell structure is  $2780\ \mu\text{m}$ . The sensor is shown with its dimensions in Fig. 1(d). Sensor chips are affixed onto the test materials using a standard hard epoxy. The compression apparatus applies loads to the test materials up to 300 kgf. To read telemetrically the strain on the test material with the metamaterial sensor chips, one antenna is used as the excitation transmitter and the other as the signal receiver. For this purpose, standard gain horn antennas are employed (shown in Fig. 1(e)).

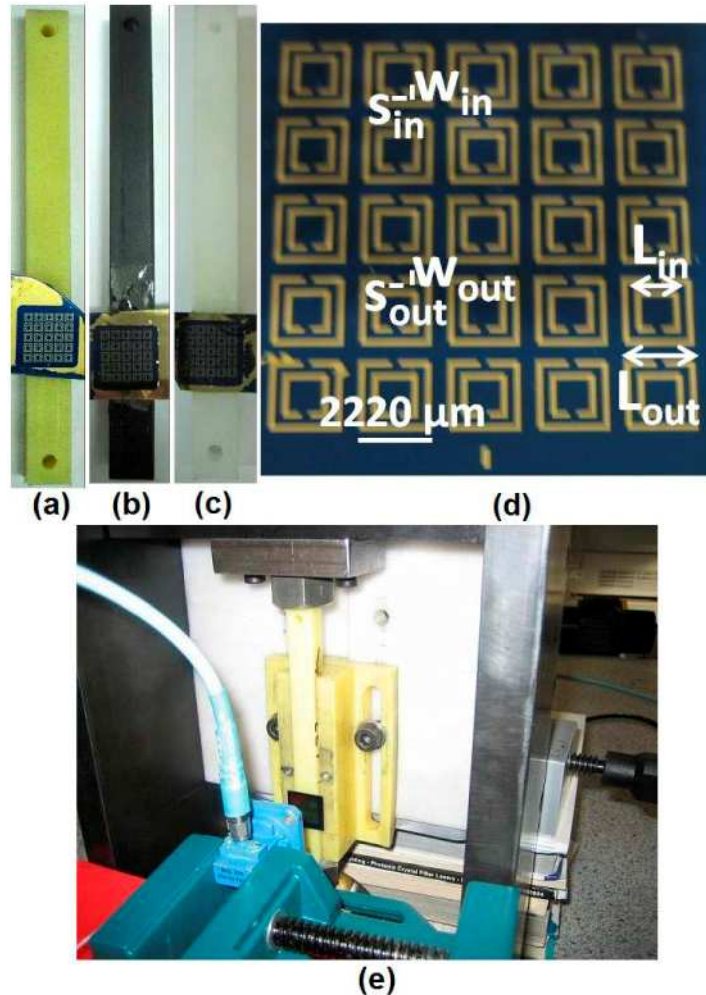


Fig. 1. The fabricated sensors fixated on different materials. The materials are (a) cast polyamide, (b) derlin and (c) polyamide. (d) The sensor shown with its dimensions. (e) Our compression setup.

We apply the external load to the test materials in a controlled manner using our compression setup and, by knowing the Young's modulus and cross-sectional area of the specimen [13], we then calculate the theoretically imposed strain assuming linear elasticity. Finally, all strain measurements obtained with our wireless strain sensors and those of the commercial wired strain gauges are compared. The wired strain gauge used in this study was acquired from Tokyo Sokki Kenkyujo Co., Ltd., Tokyo, Japan (with a 2.1 gauge factor), which is one of the best semiconductor based wired gauges. The output resistance of the wired strain gauge was obtained using a standard parameter analyzer. In the strain gauges, the application of load to the test material results in a Hall effect resistance change, and, dividing the applied stress by the Young's modulus, one can compute the applied microstrain. In all test materials, we set the working range over 2000 microstrain (for both wired measurements using the strain gauge and wireless measurements using the metamaterial chips). So, in all the cases, experimental data over 2000 microstrain are shown and compared.

For wireless measurements using the metamaterial chips, the transmission of the test material is measured when no sensor chip is attached to the test article in order to obtain the reference calibration. This measurement is repeated with the sensor under no load and then with the application of different compressive loads. Transmission spectra referenced relative

to the no sensor case is obtained as a function of the applied load. From the transmission spectra of the sensor, we obtain the operating frequencies corresponding to different levels of applied loads. Then we subtract the no load operating frequency from these operating frequencies and obtain the relative operating frequency shifts ( $\Delta f_0$ ). We obtain the operating frequency by looking at the minimum dip point in the range where we explore the shift with the applied load. Microstrain values are then obtained by dividing the applied stress by the Young's modulus for the test article. This gives the microstrain versus the relative frequency shift characteristics.

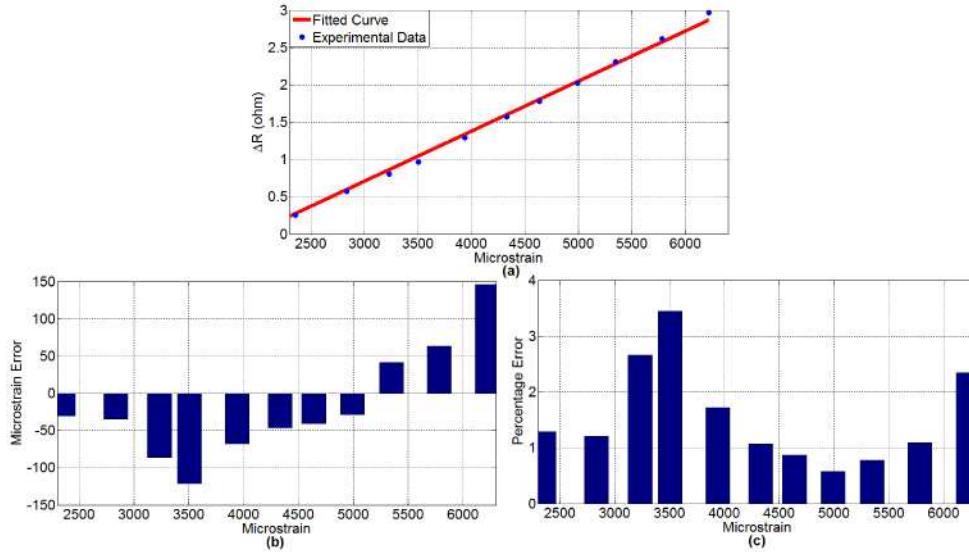


Fig. 2. Wired strain gauge measurements on cast polyamide test specimen. (a) Microstrain vs.  $\Delta R$ , (b) microstrain nonlinearity-error and (c) percentage nonlinearity-error of the wired strain gauge measurements.

Figure 2(a) shows microstrain vs.  $\Delta R$  data for the cast polyamide using the strain gauge, where  $\Delta R$  is referenced to the no load condition measured as  $351.239 \Omega$ . Here the Young's modulus of the cast polyamide is taken to be 3.0 GPa. Here we obtain a maximum microstrain nonlinearity-error of 150-microstrain given in Fig. 2(b) and a maximum nonlinearity-error of 4% given in Fig. 2(c). The measurement sensitivity of the strain gauge on the cast polyamide is  $6.708 \times 10^{-4} \Omega \text{microstrain}^{-1}$ . Figure 3(a) presents the transmission spectra of the metamaterial sensor on the cast polyamide with different applied loads changing from 28 to 271 kgf. The metamaterial sensor exhibits over a 10 dB dip in its transmission spectra where the no-load operating frequency is measured as 12.783 GHz. Figure 3(b) shows the corresponding microstrain vs.  $\Delta f_0$  characterization. The measurement sensitivity of the metamaterial sensor on the cast polyamide is 0.0543 MHz/kgf, or equivalently  $2.348 \times 10^{-3} \text{MHz} \text{microstrain}^{-1}$ . In Fig. 3(c), we see the microstrain nonlinearity-error distribution of the metamaterial sensor that has a maximum error of 500-microstrain. In Fig. 3(d) we observe a maximum percentage nonlinearity-error of 15%.

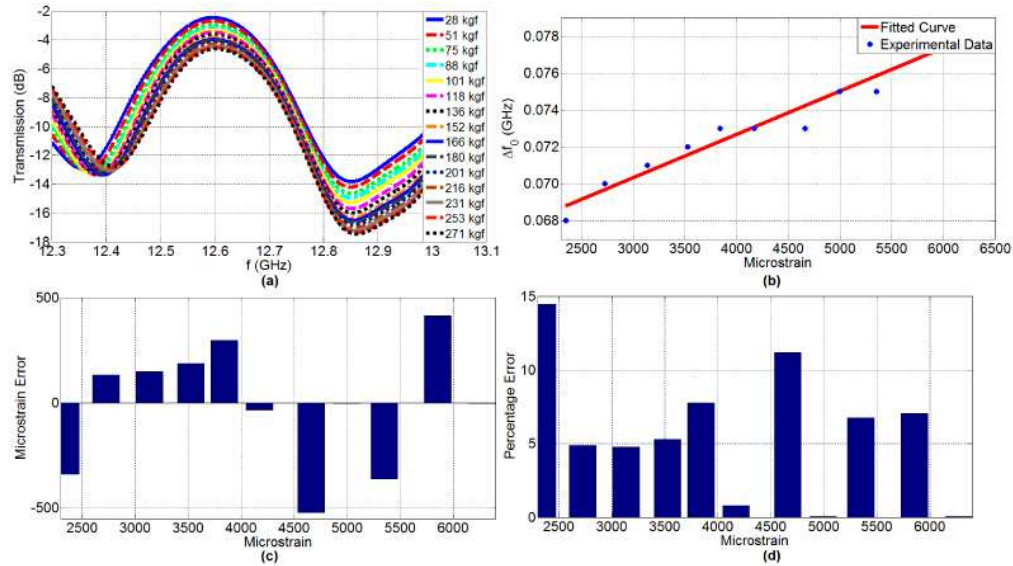


Fig. 3. Metamaterial measurements on cast polyamide stick. (a) Transmission spectra with respect to the case of no load, (b) microstrain vs.  $\Delta R$ , (c) microstrain nonlinearity-error and (d) percentage nonlinearity-error of the wireless measurements.

Figure 4 shows measurements of the wired strain gauge on the derlin test specimen (with the Young's modulus of 2.7 GPa). When we apply strain to the test article, the resistance of the wired strain gauge (whose initial resistance is  $350.783 \Omega$  under no load) changes by a few ohms. This relative change of the resistance,  $\Delta R$ , is obtained by subtracting the no load resistance from the measurements of resistances when different strains are applied. A linear microstrain vs.  $\Delta R$  characteristics is obtained (presented in Fig. 4(a)), with a maximum microstrain nonlinearity-error less than 200-microstrain (shown in Fig. 4(b)). This represents a nonlinearity-error percentage less than 4% (given in Fig. 4(c)). The measurement sensitivity of the wired gauge on the derlin is  $6.8 \times 10^{-4} \Omega \text{microstrain}^{-1}$ .

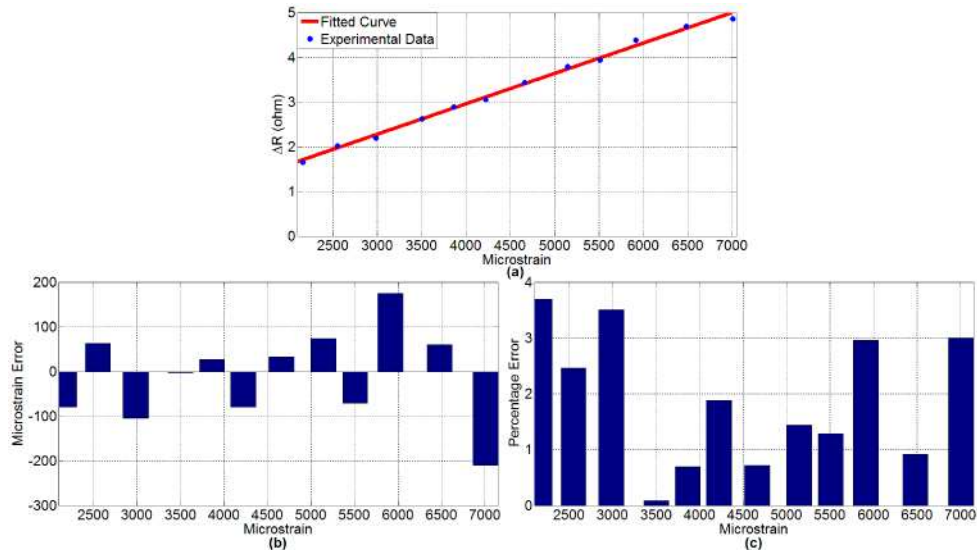


Fig. 4. Wired strain gauge measurements on derlin test specimen. (a) Microstrain vs.  $\Delta R$ , (b) microstrain nonlinearity-error and (c) percentage nonlinearity-error of the wired strain gauge measurements.

The transmission spectra of the metamaterial sensor are shown parameterized with respect to external loads applied to the derlin specimen in Fig. 5(a), where the operating frequency is measured as 12.737 GHz under no load and the observed dip is >10 dB. From these data, the microstrain vs.  $\Delta f_0$  characteristics is obtained in Fig. 5(b). The measurement sensitivity of the wireless sensor on the derlin is 0.0577 MHz/kgf, or  $2.224 \times 10^{-3} \text{ MHz microstrain}^{-1}$ . The maximum microstrain nonlinearity-error (shown in Fig. 5(c)) is 300-microstrain, which represents a maximum percentage error of 9% (given in Fig. 5(d)). From these results, we observe that the strain measurements obtained with the wireless metamaterial sensor closely approximates those obtained with the commercially available wired strain gauge. These data indicate that the wireless sensor is capable of measuring the strain remotely.

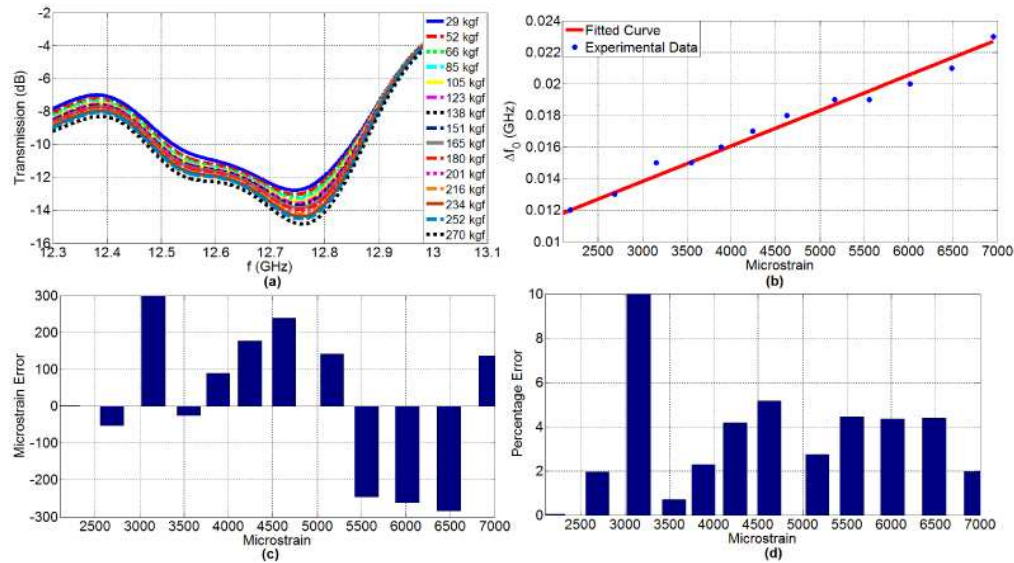


Fig. 5. Metamaterial measurements on derlin stick. (a) Transmission spectra with respect to the case of no load, (b) microstrain vs.  $\Delta R$ , (c) microstrain nonlinearity-error and (d) percentage nonlinearity-error of the wireless measurements

In Fig. 6, we show the measurement results on the polyamide stick (with the Young's modulus of 1.8 GPa) with the wired strain gauge. The no load resistance is 351.1909  $\Omega$ . The microstrain nonlinearity-error (presented in Fig. 6(b)) is less than a maximum level of 1000 microstrain, with a corresponding maximum percentage nonlinearity-error of 10% (given in Fig. 6(c)). The measurement sensitivity of the wired gauge operating on the polyamide is  $6.758 \times 10^{-4} \Omega \text{ microstrain}^{-1}$ . We also present the transmission spectra parameterized with respect to the applied loads on the polyamide specimen changing from 31 kgf to 273 kgf in Fig. 7(a). The no load operating frequency is measured as 12.710 GHz, with a local dip of >10 dB. From Fig. 7(b) the measurement sensitivity of the wireless sensor on the polyamide is obtained to be 0.119 MHz/kgf, or  $3.224 \times 10^{-3} \text{ MHz microstrain}^{-1}$ . The maximum microstrain nonlinearity-error is 1500 microstrain (as illustrated in Fig. 7(c)) and the maximum percentage nonlinearity-error is 19% (as demonstrated in Fig. 7(d)). From these results, we conclude that the surface strain can be measured telemetrically with our wireless metamaterial sensor. In addition, all these data provide de facto evidence that metamaterials can be utilized as sensors for many application areas that require measuring mechanical strain remotely.

It is important to view these results within the context of the measurement capabilities used in this investigation. For the wireless experiments, the maximum number of points that the network analyzer can obtain is limited (which is 801 in our case). We focus on the spectral region around 800 MHz to facilitate identifying the transmission minimum (operating

frequency). However, given the operating frequency of the sensor, this resolution may not be sufficient to accurately characterize the absolute local minimum. As a result, the nonlinearity-error is truly a gestalt and represents the sum of the nonlinearity-errors of the wireless sensor and the measurement system. For our wired strain gauge measurements, the measurements were taken with a parameter analyzer. Because of the resolution sufficiency of the parameter analyzer, the measured nonlinearity-error is dominated by the error of the wired strain gauge, not the error of the measurement system. To illustrate the point, if the resistance measurements were instead taken with a multimeter, there would be much more nonlinearity-error in the measurements because the multimeter's resolution is not as good as the parameter analyzer, resulting in a contribution to the overall nonlinearity-error. For our wireless strain sensor measurements, since the network analyzer's maximum collection is 801 points over the defined frequency range, this is then analogous to making the wired strain gauge measurements with a standard multimeter. Conversely, if we had the capability to take 16001 points, we would then anticipate an associated reduction in the nonlinearity-error.

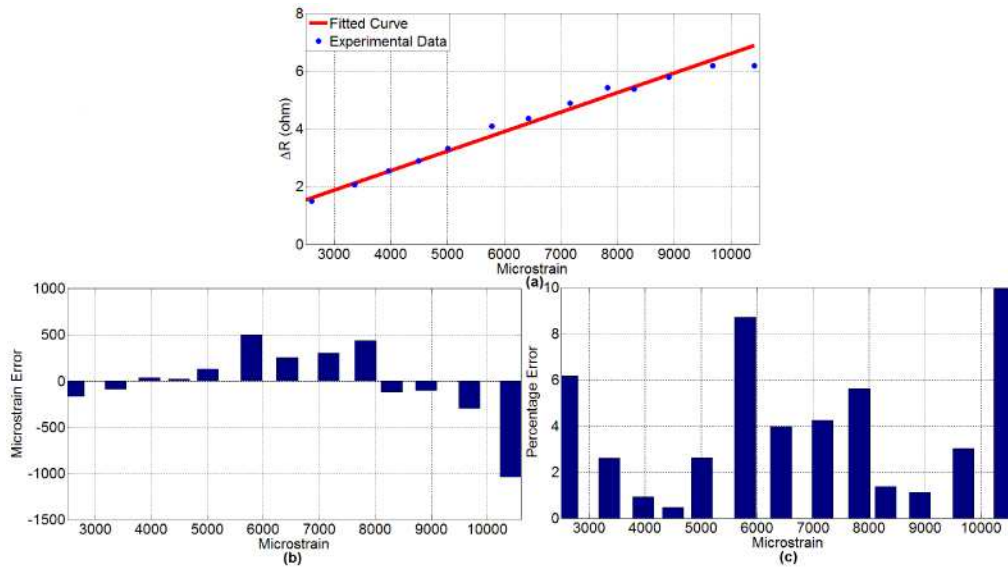


Fig. 6. Wired strain gauge measurements on polyamide test specimen. (a) Microstrain vs.  $\Delta R$ , (b) microstrain nonlinearity-error and (c) percentage nonlinearity-error of the wired strain gauge measurements.

Numerically, for the wireless sensor, the average sensitivity is found to be  $2.5987 \times 10^{-3} \text{ MHz microstrain}^{-1}$ , resulting in 384.807 microstrain resolution ( $1/(2.5987 \times 10^{-3})$ ). For the wired strain gauge, the average sensitivity is  $6.7553 \times 10^{-4} \text{ } \Omega \text{ microstrain}^{-1}$  and the minimally detectable current is  $1 \mu\text{A}$  (which corresponds to  $0.123 \Omega$ ), then we obtain 182.079 microstrain resolution ( $0.123/(6.7553 \times 10^{-4})$ ). For the wireless strain gauge, if we use a network analyzer, which can take up to 16001 points, the minimum resolution will be 1/20 of the current resolution (or 19.24 microstrain). If we also narrow down the frequency sweep band, this resolution will also be further reduced.

Finally, it is worth mentioning one important issue that relates to the thermal effects of wired strain gauges and wireless metamaterial sensors. It is well known that traditionally strain gauges that utilize the Hall effect display significant thermal drift due to their resistance dependent evolution of heat. This, in turn, can introduce significant nonlinearity-error in their measurements. Given that the metamaterial sensors are not under constant current, this effect is all but eliminated in these wireless sensors.

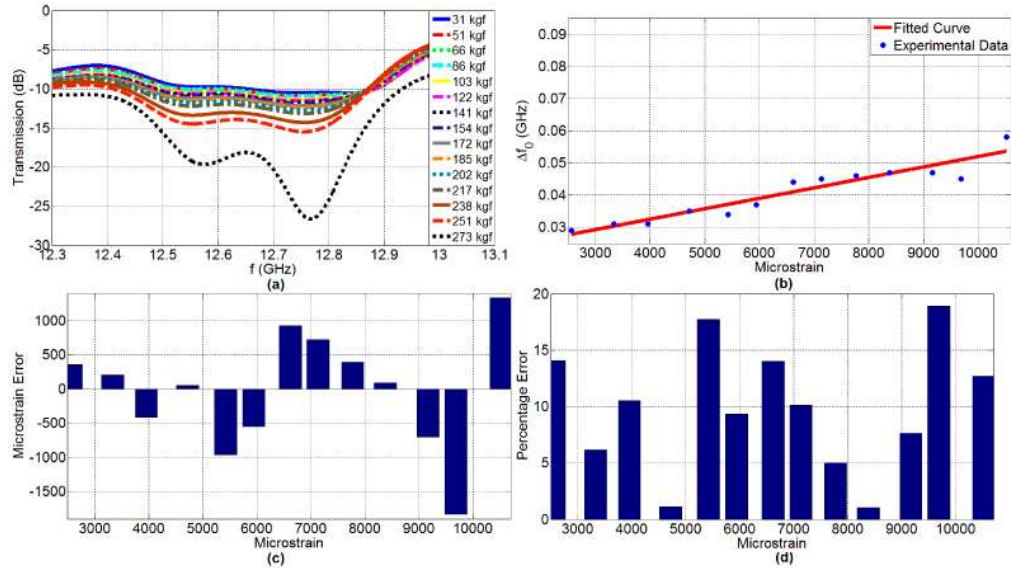


Fig. 7. Metamaterial measurements on polyamide stick. (a) Transmission spectra parameterized with respect to the case of no load, (b) microstrain vs.  $\Delta R$ , (c) microstrain nonlinearity-error and (d) the percentage nonlinearity-error of the wireless measurements.

### 3. Conclusion

In conclusion, we have experimentally showed that wireless metamaterial based strain sensors are capable of telemetrically measuring the surface strain on different materials including cast polyamide, derlin and polyamide. Because of the structural properties of the metamaterials, the wireless metamaterial sensors exhibit large frequency minima, leading to high sensitivity and low nonlinearity-errors. They exhibit more than a 10 dB dip in transmission spectra, and the nonlinearity-errors are reasonable when compared to those of the commercially available wired strain gauge, in spite of the addition of the measurement system error. The wireless sensor shows a  $c 2.5987 \times 10^{-3} \text{ MHz microstrain}^{-1}$  measurement sensitivity on the average, with a maximum nonlinearity-error of 15% in cast polyamide, 9% in derlin, and 19% in polyamide. By measuring strain telemetrically in different industrial materials, we have presented a proof-of-concept demonstration that metamaterials can be used as wireless sensors for many application areas that require measuring mechanical strain telemetrically.

### Acknowledgements

This work is supported by TÜBA-GEBİP, ESF-EURYI, and TÜBİTAK EEEAG 105E066, 105E065, 106E020, 107E088, 107E297, 109E002, and 109E004, and EU MOON 021391. This work is also supported by a subcontract from the United States National Institutes of Health (NIH) 5R01EB010035-02.